TITLE OF SYMPOSIUM: Multiaxial Fatigue and Deformation: Testing and Prediction

AUTHORS' NAMES:

Sreeramesh Kalluri[1] and Peter J. Bonacuse[2]

TITLE OF PAPER:

Cumulative Axial and Torsional Fatigue: An Investigation of Load-Type Sequencing Effects

(Paper ID # 8013)

AUTHORS' AFFILIATIONS:

[1]Senior Research Engineer, Ohio Aerospace Institute, NASA Glenn Research Center, Cleveland, Ohio.

[2]Materials Research Engineer, Army Research Laboratory, NASA Glenn Research Center, Cleveland, Ohio.

ABSTRACT: Cumulative fatigue behavior of a wrought cobalt-base superalloy, Haynes 188 was investigated at 538°C under various single-step sequences of axial and torsional loading conditions. Initially, fully-reversed, axial and torsional fatigue tests were conducted under strain control at 538°C on thin-walled tubular specimens to establish baseline fatigue life relationships. Subsequently, four sequences (axial/axial, torsional/torsional, axial/torsional, and torsional/axial) of two load-level fatigue tests were conducted to characterize both the load-order (high/low) and load-type sequencing effects. For the two load-level tests, summations of life fractions and the remaining fatigue lives at the second load-level were computed by the Miner's Linear Damage Rule (LDR) and a nonlinear Damage Curve Approach (DCA). In general, for all four cases predictions by LDR were unconservative. Predictions by the DCA were within a factor of two of the experimentally observed fatigue lives for a majority of the cumulative axial and torsional fatigue tests.

KEYWORDS: axial fatigue, cumulative fatigue, cyclic hardening, damage curve approach, life prediction, linear damage rule, load-type sequencing, torsional fatigue

Nomenclature

b, c	Exponents of elastic and inelastic strain range-life relations
n	Number of applied cycles at a load level in a cumulative fatigue test
B, C	Coefficients of elastic and inelastic strain range-life relations
MF	Multiaxiality factor
N	Number of cycles
TF	Triaxiality factor
ε	Engineering axial strain

γ Engineering shear strain

ν Frequency of the waveform in a fatigue test

Δ Denotes range of a variable

σ Axial stress

τ Shear stress

Subscripts

1 First load level in a two-load level cumulative fatigue test

2 Second load level in a two-load level cumulative fatigue test

el elastic

in inelastic

m mean value

f failure

A Axial

T Torsional

I First principal

II Second principal

III Third principal

Introduction

Accumulation of damage in materials subjected to fatigue under multiple load levels and estimation of cyclic life under cumulative fatigue has been the subject of investigation for the past 75 years [1-13]. In these cumulative fatigue investigations materials have been typically subjected to the same load-type (for example, axial tension/compression [3,13], torsion [4,8,9],

or rotating bending [5,6]), albeit to different magnitudes, during the multiple loading levels. In engineering design, fatigue life under cumulative fatigue loading conditions is commonly estimated with a Linear Damage Rule (LDR) [1-3], primarily due to its simplicity, associated ease of implementation, and lack of proven applicability of alternative rules. However, inadequacy of the LDR to properly account for the load order effects (either high/low or low/high for a given load-type) has been well documented in the literature [6-13]. Within a specified load-type, the high/low load ordering typically generates a sum of life fractions less than unity, whereas the low/high load ordering typically generates a sum of life fractions greater than unity. Several nonlinear damage accumulation models [6-12] have been developed to overcome the disadvantages of the LDR for predicting fatigue lives of materials subjected to multiple load levels. Most of the nonlinear damage accumulation models capture the well-known load order effects adequately for a given load-type under cumulative cyclic loading conditions.

The cumulative fatigue behavior of materials under dissimilar load-types could potentially be different from that under a single load-type due to either a lack of interaction or a potential synergistic interaction between the deformation and damage modes and their orientation associated with the two load-types. Investigations involving cumulative fatigue of materials with dissimilar load-types are relatively recent in comparison to those involving the same load-type [14-22]. During the past 15-20 years, researchers have investigated accumulation of fatigue damage in materials under dissimilar load-types such as 1) tension/compression, torsion, and proportional and nonproportional combined axial-torsional loads [14-17, 19-22] and 2) torsion and bending [18]. For cumulative fatigue involving axial and torsional loading conditions most of the previous studies have been conducted with 1) the same equivalent strain range [14,17,19,20], 2) the same fatigue lives [16], or 3) with the same equivalent damage [21].

Equivalency in terms of strain range, fatigue life, or damage is selected primarily to separate the load order effects from the load-type sequencing effects. In general, under equivalent loading conditions, cyclic tension/compression followed by cyclic torsion type load sequencing has been found to be more benign than that predicted by LDR (for example, with a sum of cycle fractions greater than unity), whereas the load-type sequencing of cyclic torsion followed by cyclic tension/compression has been reported to be more damaging than that estimated by LDR (with a sum of cycle fractions less than or equal to unity) [16,17,19,20]. However, in a few investigations [19-21] it has been reported that the load-type sequencing of cyclic tension/compression followed by cyclic torsion is more detrimental than cyclic torsion followed by cyclic tension/compression. This reversal in load-type sequencing effects has been attributed to differences in the cracking patterns of materials that are caused by temperature dependent environmental effects (for example, oxidation) and inherent differences in microstructures. Cumulative fatigue investigations that considered load order as well as load-type sequencing effects under cyclic axial and torsional loads are rather limited in number [15,22]. As far as fatigue life estimation is concerned, noticeable deviations from the LDR have been reported in both studies.

The objective of the present study was to evaluate the effects of both load-type sequencing and high/low load ordering under cumulative axial and torsional loading conditions. A test program was designed to investigate the cumulative fatigue behavior of a representative high temperature superalloy under various sequences of axial and torsional loading conditions. The wrought cobalt-base superalloy, Haynes 188 was selected for this purpose. Examples of the many applications of this superalloy include the cryogenic oxygen carrying tubes in the main injector of the reusable space shuttle main engine and the combustor liner in the T-800 turboshaft

engine for the RAH-66 Comanche helicopter. Axial, torsional, and combined axial-torsional fatigue behavior of Haynes 188 under isothermal (316 and 760°C) and thermomechanical (316 to 760°C) loading conditions on a single heat of the superalloy was previously documented by the authors [23-27]. In the current investigation, axial and torsional fatigue tests were conducted at 538°C on material from another heat of Haynes 188 to establish baseline fatigue lives. Subsequently four sequences (axial/axial, torsional/torsional, axial/torsional, and torsional/axial) of two load-level (single-step) fatigue tests were conducted (same heat as that used for the baseline tests) at 538°C to characterize the cumulative fatigue behavior of the superalloy. For the two load-level tests, summations of life fractions and the remaining fatigue lives at the second load-level were estimated with two models, LDR [1-3] and the nonlinear Damage Curve Approach (DCA) [7,10]. This paper summarizes details of the test program, results from the axial and torsional cumulative fatigue tests, and predictive capabilities of the models.

Material and Specimens

Solution annealed, hot rolled, cobalt-base superalloy, Haynes 188, was supplied by the manufacturer in the form of round bars with a diameter of 50.8 mm (heat number: 1-1880-6-1714). The composition of the superalloy in weight percent was as follows: <0.002 S, 0.003 B, <0.005 P, 0.09 C, 0.35 Si, 0.052 La, 0.8 Mn, 1.17 Fe, 14.06 W, 22.11 Cr, 22.66 Ni, balance Co. Thin-walled tubular specimens with nominal inner and outer diameters of 22 and 26 mm, respectively, in the straight section (41mm) and an overall length of 229 mm were machined from the bar stock. Bores of the tubular specimens were finished with a honing operation and the external surfaces of the specimens were polished. Additional details on machining of tubular specimens are available in Ref. [28]. In the middle of the straight section of the tubular

specimen, two indentations (25 mm apart and 80 μm deep) were pressed with a fixture to define the gauge section and to positively locate the extensometer probes. Average values of the elastic modulus, shear modulus, and poisson's ratio for Haynes 188 at 538°C were 190 GPa, 73 GPa, and 0.3 respectively.

Experimental Details

All the tests were performed in an axial-torsional fatigue test system [27] equipped with a personal computer and a data acquisition system. Tubular specimens were heated to the test temperature of 538°C in air with a three-coil fixture [29] connected to a 15 kW induction heating unit. Specimen temperature in the gauge section was measured with a noncontacting optical temperature measurement device. Thermocouples spot-welded in the shoulder regions of the specimens were used to control and monitor the temperature during fatigue tests. Axial and engineering shear strains within the gauge section of each specimen were measured with a water-cooled, axial-torsional extensometer. Test control software written in C language was used to generate triangular, axial and torsional command waveforms at the appropriate frequencies for the strain-controlled fatigue tests. For each axial and torsional fatigue test, test control software increased the strain to the full amplitude by increasing the strain increments linearly over 10 cycles. For axial strain-controlled fatigue tests, the torsional servocontroller was in load-control at zero torque and for torsional strain-controlled fatigue tests, the axial servocontroller was in load-control at zero load. In the case of cumulative fatigue tests with two load-levels, after completing the required number of cycles at the first load-level, test control software decreased the strain amplitude to zero by reducing the strain increments linearly over 10 cycles. This procedure was necessary to return the material to an approximately zero stress and zero strain

state in a carefully controlled manner. Software was also used to acquire axial and torsional load, strain, and stroke data at logarithmic intervals in cycles and to shutdown each test in a controlled manner. For axial and torsional fatigue tests, failure was defined as a 10% load-drop from a previously recorded cycle. If a specimen did not fail after 250,000 cycles, then that test was declared a runout.

Results

Baseline Axial and Torsional Fatigue Tests

Fully reversed, strain-controlled, axial and torsional fatigue tests were conducted at 538°C to establish baseline fatigue data for the subsequent cumulative fatigue tests. Axial and torsional fatigue data obtained from near half-life cycles are listed in Tables 1 and 2, respectively. For both axial and torsional tests at higher strain ranges a frequency of 0.1 Hz was used, whereas at lower strain ranges a frequency of 0.5 Hz was used. Lowering of the frequency at higher strain ranges was necessary to achieve adequate control of the fatigue test in the presence of 'serrated yielding' [30] exhibited by Haynes 188 at 538°C [31]. Slight compressive mean stresses were observed in all the axial fatigue tests, whereas no appreciable mean stresses were noticed in the torsional fatigue tests. In a majority of the torsional fatigue tests, axial strain ratchetting in the positive direction was observed. Such axial strain ratchetting in materials subjected to torsional loading was reported by other investigators [32-35] and was also observed in Haynes 188 at 760°C [36]. However, for the tests conducted in the present study, magnitudes of the mean axial ratchetting strains near half-lives were either less than or of the same order as the equivalent imposed engineering shear strains. In a separate study [37] also conducted on Haynes 188 no significant influence of mean axial strain, either tensile or compressive, was observed on the axial fatigue life of the superalloy.

In the baseline tests, orientation of the crack(s) that lead to specimen failure was nearly perpendicular to the maximum normal stress in the axial fatigue tests, whereas in the torsional fatigue tests the crack orientation was always parallel to one of the two maximum shear directions (Tables 1 and 2). Axial and torsional fatigue life relations (Eqs. 1 and 2) were computed by separating the total strain range for each test into elastic and inelastic components (Tables 1 and 2), and subsequently performing a regressions between logarithms of the strain range components and the fatigue lives. Fatigue data from the runout tests were omitted while computing the life relationships. Constants for the axial and torsional life relationships are shown in Table 3.

$$\Delta\varepsilon = B(N_f)^b + C(N_f)^c \qquad \textbf{(Eq. 1)}$$

$$\Delta\gamma = B_T(N_f)^{b_T} + C_T(N_f)^{c_T} \qquad \textbf{(Eq. 2)}$$

Axial and torsional fatigue data and the corresponding life relationships are plotted in Figs. 1 and 2, respectively. Note that for Haynes 188 at 538°C, the slopes of the elastic and inelastic life relations for the axial and torsional loading conditions are very similar. Axial and torsional fatigue data are compared by using von Mises equivalent strain range ($\Delta\varepsilon_{eq} = \Delta\gamma/\sqrt{3}$) in Fig. 3. Most of the torsional fatigue data fall near the axial fatigue curve. The torsional fatigue life relationship was estimated from the axial fatigue life relationship by the Modified Multiaxiality Factor (MMF) Approach (Eqs. 3 and 4).

$$\Delta\varepsilon_{eq} = \left(\frac{B}{MF^{b/c}}\right)(N_f)^b + \left(\frac{C}{MF}\right)(N_f)^c \qquad \textbf{(Eq. 3)}$$

where,

$$MF = \left(\frac{1}{2 - TF}\right); TF \le 1$$

$$MF = TF; TF \ge 1 \qquad \text{(Eq. 4)}$$

$$TF = \left(\frac{\sigma_I + \sigma_{II} + \sigma_{III}}{\frac{\sqrt{(\sigma_I - \sigma_{II})^2 + (\sigma_{II} - \sigma_{III})^2 + (\sigma_{III} - \sigma_I)^2}}{\sqrt{2}}} \right)$$

This approach was previously used to estimate torsional fatigue behavior from axial fatigue life relationships of Haynes 188 at 316 and 760°C [24,25]. For torsion ($\sigma_I = -\sigma_{III}$ and $\sigma_{II} = 0$; TF = 0; and MF = 0.5), the estimated torsional fatigue life relation from Eqs. 3 and 4 forms an upper bound to the experimentally observed torsional fatigue data at 538°C (Fig. 3).

Four nominal strain ranges, two each for axial ($\Delta\varepsilon_1 = 0.02$ & $\Delta\varepsilon_2 = 0.0067$) and torsional ($\Delta\gamma_1 = 0.035$ & $\Delta\gamma_2 = 0.012$) loading conditions, were selected for the subsequent cumulative fatigue tests. Duplicate tests were conducted in the baseline test program to evaluate repeatability of the cyclic deformation behavior and to provide a more accurate estimate of the fatigue life for each test condition. The evolution of cyclic axial and shear stresses are plotted in Fig. 4 for the baseline axial and torsional tests. In each of these tests, Haynes 188 exhibited cyclic hardening for a majority of the life with a slight softening towards the end of the test. No significant differences were observed between the cyclic hardening behaviors of the duplicate tests. For a given cyclic loading condition, scatter in fatigue life typically exhibits a log-normal distribution. Therefore, geometric mean lives (arithmetic means of the logarithms of fatigue lives) of the duplicated axial and torsional baseline fatigue tests were used to design the

cumulative fatigue test matrices. The calculated geometric mean lives for the four axial and torsional fatigue loading conditions were as follows: N_{1A} = 825 cycles, N_{2A} = 39, 255 cycles, N_{1T} = 1, 751 cycles, and N_{2T} = 58, 568 cycles.

Cumulative Fatigue Tests

Four types of two load-level, axial and torsional cumulative fatigue tests were conducted to quantify the load-order as well as load-type sequencing effects. The cumulative fatigue tests involving load-order effects (high/low) without load-type sequencing effects were as follows: 1) axial/axial and 2) torsional/torsional. Cumulative fatigue tests involving both load-order (high/low) and load-type (axial and torsional) sequencing effects were as follows: 1) axial/torsional and 2) torsional/axial. For each type of two load-level test, four different life fractions (n_1/N_1 = 0.1, 0.2, 0.4 & 0.6) at the first load-level were investigated. All the cumulative fatigue tests were started at the first load-level and after completing the required number of cycles the remainder of the test was carried out to failure at the second load-level. Axial and torsional interaction fatigue data obtained from the near middle cycle for each load segment are listed in Table 4. In all cumulative fatigue tests, after the completion of the first load segment any existing mean strains (for example, axial ratchetting strain due to cyclic torsional loading) were rezeroed before starting the second load segment. In the axial/axial and torsional/axial cumulative fatigue tests orientation of the crack(s) leading to failure of the specimens were nearly perpendicular to the maximum normal stress direction induced by the axial loads (Table 4). In the case of torsional/torsional fatigue tests cracks were oriented along both of the maximum shear stress planes. Axial/torsional cumulative fatigue testing resulted in crack orientations both along planes of maximum shear stress and perpendicular to the maximum normal stress direction.

The cyclic hardening behavior exhibited by Haynes 188 during the different types of axial and torsional cumulative fatigue tests is shown in Figs. 5(a) to (d). The corresponding baseline cyclic hardening behaviors are also included for comparison. Note that the cyclic hardening behavior from the second load-level alone is included in each of these plots. In all the cumulative fatigue tests, Haynes 188 cyclically softened during the latter segments of the two load-level tests. This was to be expected because the material was cyclically hardened during the first load segments, which were applied at much higher strain ranges compared to the lower strain ranges in the second load segments. In axial/axial and torsional/axial cumulative fatigue tests, hardening of the material during the first load segments resulted in the second segment axial strain range levels to be slightly lower than the intended nominal value of $\Delta\varepsilon_2 = 0.0067$ (Table 4).

Applied and remaining life fractions in the two load-level axial and torsional cumulative tests are shown in Figs. 6 (a) to (d). In all the figures, corresponding predictions from the LDR (Eq. 5) and the nonlinear DCA (Eq. 6) are also included.

$$\left(\frac{n_2}{N_2}\right) = 1 - \left(\frac{n_1}{N_1}\right) \qquad \textbf{(Eq. 5)}$$

$$\left(\frac{n_2}{N_2}\right) = 1 - \left(\frac{n_1}{N_1}\right)^{\left(\frac{N_1}{N_2}\right)^{0.4}} \qquad \textbf{(Eq. 6)}$$

Applied and summations of the life fractions observed in the two load-level axial and torsional cumulative fatigue tests and the corresponding predictions from the LDR and the nonlinear DCA are listed in Table 5 and are also shown in Figs. 7(a) to (d). The baseline fatigue lives used for

the LDR and the DCA computations are indicated in the figures 6 and 7. In most instances, the baseline fatigue lives (N_{1A}, N_{1T}, N_{2A}, and N_{2T}) were obtained directly from the geometric mean fatigue lives as mentioned earlier (Figs. 6 (a) to (c) and Figs. 7(a) to (c)). In the case of torsional/axial cumulative tests, however, N_{2A} value corresponding to the lower than nominal axial strain range was calculated from Eq. 1 (Figs. 6(d) and 7 (d)).

For axial/axial cumulative fatigue tests, which primarily involve load-order (high/low) interaction effect within axial loading, the curve from the DCA predicted the trend in the data very well, whereas the predictions by the LDR were unconservative (Fig. 7(a)). In the case of torsional/torsional cumulative fatigue tests, which involves load-order interaction effect within torsional loading, predictions by the LDR were unconservative in 3 out of 4 instances (Fig. 7(b)) and the DCA was able to only approximate the general trend of the data. In fact for two data points predictions by DCA were conservative and for the remaining data points they were unconservative. The cumulative fatigue behavior under torsional loading will be discussed further in the following section. In the axial/torsional and torsional/axial cumulative fatigue tests, which consider both the high/low load-ordering and load-type sequencing effects, the DCA was able to closely predict the trends of the data and the LDR was unconservative in both instances (Figs. 7(c) and (d)). Experimentally observed remaining fatigue lives at the second load-level and corresponding predictions by the LDR and the DCA are compared in Figs. 8 (a) and (b), respectively, for the cumulative axial and torsional fatigue tests. For a majority of the tests predictions by the LDR were unconservative by more than a factor of two. Predicted remaining fatigue lives by the DCA were generally within a factor of two of the observed fatigue lives with a few exceptions.

Discussion

The baseline torsional fatigue data, when compared on the basis of von Mises equivalent strain range, fall slightly above the axial fatigue data (Fig. 3). This observation indicates that for Haynes 188 at 538°C, torsion is a slightly more benign type of loading compared to axial loading. The predictions by the MMF approach, as indicated earlier, form a close upper bound to the torsional fatigue data. In the absence of any torsional fatigue data, the MMF approach can be used for Haynes 188 to estimate the torsional fatigue lives from the axial fatigue life relationship at the appropriate temperature.

Axial/axial and torsional/torsional cumulative fatigue tests were performed mainly to investigate the high/low load ordering effects without load-type sequencing. The axial/axial cumulative fatigue behavior of Haynes 188 was predicted accurately by the DCA (Fig. 7(a) and Table 5), whereas the torsional/torsional behavior did not closely confirm to the predictions by either LDR or DCA (Fig. 7(b) and Table 5). The orientation of crack(s) did not vary significantly in the axial/axial tests (Table 4). In the torsional/torsional tests, the orientation of the crack(s) leading to the failure of the specimens shifted from one maximum shear plane (0° or parallel to the specimen's axis) to another (90° or perpendicular to the specimen's axis) as the life fraction of the first load segment was increased from 0.1 to 0.6 (Table 4). It is also interesting to note that the predictions by DCA are conservative for $n_1/N_1 = 0.1$ & 0.2 and unconservative for $n_1/N_1 = 0.4$ & 0.6. Cracking pattern appears to influence the cumulative fatigue behavior of Haynes 188 under torsion. Wood and Reimann [4] also observed some unusual cumulative fatigue behavior while testing brass and copper under torsion. In their study, the unusual behavior was attributed to a change in the damage mechanisms of the materials [4]. Additional torsional/torsional cumulative fatigue tests on Haynes 188 at closer n_1/N_1 intervals are

required to characterize this behavior in a systematic manner. Comprehensive microstructural examination of the material subjected to interrupted tests could determine whether different damage mechanisms are involved.

Axial/torsional and torsional/axial tests were conducted to understand the influences of both high/low load ordering and load-type sequencing on the cumulative fatigue behavior of Haynes 188. The predictions by the DCA for both types of cumulative fatigue tests closely followed the experimental results even though there were some variations in the failure crack orientations (Table 4). Typically, under equivalent loading conditions, load-type sequencing effect results in a total life fraction of greater than unity for either the axial/torsional or torsional/axial cumulative fatigue tests [16, 17, 19-21]. In the present study total life fractions from both the axial/torsional and the torsional/axial cumulative fatigue tests were less than unity (Figs. 7 (c) & (d) and Table 5). This result clearly indicated that for Haynes 188 at 538°C and the test conditions investigated in this study the high/low load ordering effect was much stronger than the load-type sequencing effect. Hua and Socie [15] and Hua and Fernando [22] also observed similar dominance of load ordering effects on the cumulative fatigue lives of other materials. However, load-type sequencing can significantly influence the cumulative fatigue behavior of a material when load-ordering effect is either eliminated by careful design of the cumulative fatigue experiments (equivalent strain range, or equal cyclic lives or equivalence in damage) or minimized in comparison to the load-type sequencing effect [14, 16, 17, 19-21].

Summary

Cumulative fatigue behavior of a wrought cobalt-base superalloy, Haynes 188 was investigated under axial and torsional loading conditions at 538°C. Four different types of two load-level (single-step), high/low load ordering, cumulative fatigue tests were performed with

(axial/torsional and torsional/axial) and without load-type sequencing (axial/axial and torsional/tosional). The cyclic lives in the cumulative fatigue tests were estimated with the LDR and the DCA. Important issues identified from this study are summarized as follows:

1) In baseline fatigue tests, orientation of dominant crack(s) was nearly perpendicular to the maximum normal stress direction under axial loading, whereas under torsional loading the orientation was always parallel to the maximum shear stress planes.
2) For the axial/axial and torsional/torsional cumulative fatigue tests, which involve only high/low ordering effects and no load-type sequencing effects, the summations of life fractions were less than unity in all except one torsional/torsional test. This confirmed the presence of a high/low order effect in Haynes 188 superalloy. Even in the case of axial/torsional and torsional/axial cumulative fatigue tests, which potentially contain both the high/low ordering and load-type sequencing effects, the summations of life fractions were less than unity in all the tests. This essentially indicated that for the test conditions evaluated in this study high/low load ordering effect was more predominant than the load-type sequencing effects.
3) In the cumulative fatigue tests, predicted summations of the life fractions by the LDR were unconservative for all except one torsional/torsional test, whereas those predicted by the DCA closely matched the experimental data for axial/axial, axial/torsional, and torsional/axial tests. In the case of torsional/torsional tests the DCA was only able to predict the general trend in the data.
4) Remaining cyclic life predictions by the LDR were unconservative by more than factor of two for a majority of the cumulative axial and torsional fatigue tests and corresponding

predictions by the DCA were generally within a factor of two of the experimental data with few exceptions.

Acknowledgment

Valuable technical discussions with Dr. Gary R. Halford (NASA Glenn Research Center) and the diligent efforts of Mr. Christopher S. Burke (Dynacs Engineering Company, Inc.) in the High Temperature Fatigue and Structures Laboratory are gratefully acknowledged.

References

[1] Palmgren, A., "Die Lebensdauer von Kugellagern," *Zeitschrift des Vereinesdeutscher Ingenierure*, Vol. 68, No. 14, April 1924, pp. 339-341 (The Service Life of Ball Bearings, NASA Technical Translation of German Text, NASA TT 1-13460, 1971).

[2] Langer, B. F., "Fatigue Failure from Stress Cycles of Varying Amplitude," *Journal of Applied Mechanics*, Vol. 4, No. 3, September 1937, (*Transactions of the American Society of Mechanical Engineers*, Vol. 59, 1937), pp. A160-A162.

[3] Miner, M. A., "Cumulative Damage in Fatigue," *Journal of Applied Mechanics*, Vol. 12, No. 3, September 1945, (*Transactions of the American Society of Mechanical Engineers*, Vol. 67, 1945), pp. A159-A164.

[4] Wood, W. A. and Reimann, W. H., "Observations on Fatigue Damage Produced by Combinations of Amplitudes in Copper and Brass," *Journal of the Institute of Metals*, Vol. 94, 1966, pp. 66-70.

[5] Manson, S. S., Nachtigall, A. J., Ensign, C. R., and Freche, J. C., "Further Investigation of a Relation for Cumulative Fatigue Damage in Bending," *Journal of Engineering for Industry*, 1965, pp. 25-35.

[6] Manson, S. S., Freche, J. C., and Ensign, C. R. "Application of a Double Linear Damage Rule to Cumulative Fatigue," *Fatigue Crack Propagation*, ASTM STP 415, American Society for Testing and Materials, 1967, pp. 384-412.

[7] Manson, S. S. and Halford, G. R., "Practical Implementation of the Double Linear Damage Rule and Damage Curve Approach for Treating Cumulative Fatigue Damage," *International Journal of Fracture*, Vol. 17, No. 2, 1981, pp. 169-192.

[8] Bui-Quoc, T., "Cumulative Damage with Interaction Effect due to Fatigue Under Torsion Loading," *Experimental Mechanics*, 1982, pp. 180-187.

[9] Miller, K. J. and Ibrahim, M. F. E., "Damage Accumulation During Initiation and Short Crack Growth Regimes," *Fatigue of Engineering Materials and Structures*, Vol. 4, No. 3, 1981, pp. 263-277.

[10] Manson, S. S., and Halford, G. R., "Re-examination of Cumulative Fatigue Damage Analysis -- An Engineering Perspective", *Engineering Fracture Mechanics,* Vol. 25, Nos. 5/6, 1986, pp. 539-571.

[11] Golos, K. and Ellyin, F., "Generalization of Cumulative Damage Criterion to Multilevel Cyclic Loading," *Theoretical and Applied Fracture Mechanics*, Vol. 7, 1987, pp. 169-176.

[12] Chaboche, J. L. and Lesne, P. M., "A Non-Linear Continuous Fatigue Damage Model," *Fatigue and Fracture of Engineering Materials and Structures*, Vol. 11, No. 1, 1988, pp. 1-17.

[13] McGaw, M. A., Kalluri, S., Moore, D., and Heine, J., "The Cumulative Fatigue Damage Behavior of Mar-M 247 in Air and High Pressure Hydrogen," *Advances in Fatigue*

Lifetime Predictive Techniques: Second Volume, ASTM STP 1211, M. R. Mitchell and R. W. Landgraf, Eds., American Society for Testing and Materials, 1993, pp. 117-131.

[14] Miller, K. J., and Brown, M. W., "Multiaxial Fatigue: A Brief Review," *Fracture 84*, Proceedings of the Sixth International Conference on Fracture, 1984, New Delhi, India, Pergamon Press, pp. 31-56

[15] Hua, C. T. and Socie, D. F., "Fatigue Damage in 1045 Steel Under Variable Amplitude Biaxial Loading," *Fatigue and Fracture of Engineering Materials and Structures*, Vol. 8, No. 2, 1985, pp. 101-114.

[16] Miller, K. J., "Metal Fatigue – Past, Current, and Future," Proceedings of the Institution of Mechanical Engineers, Vol. 205, 1991, pp. 1-14.

[17] Robillard, M. and Cailletaud, G. "'Directionally Defined Damage' in Multiaxial Low-Cycle Fatigue: Experimental Evidence and Tentative Modelling," *Fatigue Under Biaxial and Multiaxial Loading*, ESIS10, (Edited by K. Kussmaul, D. McDiarmid, and D. Socie), 1991, Mechanical Engineering Publications, London, pp. 103-130.

[18] Harada, S. and Endo, T. "On the Validity of Miner's Rule under Sequential Loading of Rotating Bending and Cyclic Torsion," *Fatigue Under Biaxial and Multiaxial Loading*, ESIS10, (Edited by K. Kussmaul, D. McDiarmid, and D. Socie), 1991, Mechanical Engineering Publications, London, pp. 161-178.

[19] Weiss, J.and Pineau, A., "Continuous and Sequential Multiaxial Low-Cycle Fatigue Damage in 316 Stainless Steel," *Advances in Multiaxial Fatigue*, ASTM STP 1191, D. L. McDowell and R. Ellis, Eds., American Society for Testing and Materials, 1993, pp. 183-203.

[20] Weiss, J.and Pineau, A., "Fatigue and Creep-Fatigue Damage of Austenitic Stainless Steels under Multiaxial Loading," *Metallurgical Transactions A*, Vol. 24A, 1993, pp. 2247-2261.

[21] Lin, H., Nayeb-Hashemi, H., and Berg, C. A., "Cumulative Damage Behavior of Anisotropic Al-6061-T6 as a Function of Axial-Torsional Loading Mode Sequence," *Journal of Engineering Materials and Technology*, Vol. 116, 1994, pp. 27-34.

[22] Hua, G. and Fernando, U. S., "Effect of Non-Proportional Overloading on Fatigue Life," *Fatigue and Fracture of Engineering Materials and Structures*, Vol. 19, No. 10, 1996, pp. 1197-1206.

[23] Kalluri, S. and Bonacuse, P. J., "In-Phase and Out-of-Phase Axial-Torsional Fatigue Behavior of Haynes 188 Superalloy at 760°C," *Advances in Multiaxial Fatigue*, ASTM STP 1191, D. L. McDowell and J. R. Ellis, Eds., American Society for Testing and Materials, 1993, pp. 133-150.

[24] Kalluri, S., and Bonacuse, P. J., "Estimation of Fatigue Life under Axial-Torsional Loading," *Material Durability/Life Prediction Modeling: Materials for the 21st Century*, PVP-Vol. 290, S. Y. Zamrik and G. R. Halford, Eds., American Society of Mechanical Engineers, 1994, pp. 17-33.

[25] Bonacuse, P. J. and Kalluri, S., "Elevated Temperature Axial and Torsional Fatigue Behavior of Haynes 188," *Journal of Engineering Materials and Technology*, Vol. 117, April 1995, pp. 191-199.

[26] Bonacuse, P. J. and Kalluri, S., "Axial-Torsional, Thermomechanical Fatigue Behavior of Haynes 188 Superalloy," *Thermal Mechanical Fatigue of Aircraft Engine Materials*,

AGARD-CP-569, Advisory Group for Aerospace Research & Development, Neuilly-sur-Seine, France, 1996, pp. 15-1 – 15-10.

[27] Kalluri, S., and Bonacuse, P. J., "An Axial-Torsional, Thermomechanical Fatigue Testing Technique," *Multiaxial Fatigue and Deformation Testing Techniques*, ASTM STP 1280, S. Kalluri and P. J. Bonacuse, Eds., American Society for Testing and Materials, 1997, pp. 184-207.

[28] Bonacuse, P. J. and Kalluri, S., "Axial-Torsional Fatigue: A Study of Tubular Specimen Thickness Effects," *Journal of Testing and Evaluation, JTEVA*, Vol. 21, No. 3, 1993, pp. 160-167.

[29] Ellis, J. R., and Bartolotta, P.A., "Adjustable Work Coil Fixture Facilitating the Use of Induction Heating in Mechanical Testing," *Multiaxial Fatigue and Deformation Testing Techniques*, ASTM STP 1280, S. Kalluri and P. J. Bonacuse, Eds., American Society for Testing and Materials, 1997, pp. 43-62.

[30] Bhanu Sankara Rao, K., Kalluri, S., Halford, G. R., McGaw, M. A., "Serrated Flow and Deformation Substructure at Room Temperature in Inconel 718 Superalloy during Strain Controlled Fatigue," *Scripta Metallurgica et Materialia*, Vol. 32, No. 4, 1995, pp. 493-498.

[31] Bhanu Sankara Rao, K., Castelli, M. G., Allen, G. P., and Ellis, J. R., "A Critical Assessment of the Mechanistic Aspects in Haynes 188 during Low-Cycle Fatigue in the Rnage 25°C to 1000°C," *Metallurgical and Material Transactions A*, Vol. 28A, 1997, pp. 347-361.

[32] Poynting, J. H., "On Pressure Perpendicular to the Shear Planes in Finite Shears, and on the Lengthening of Loaded Wires when Twisted," *Proceedings of the Royal Society, London, Series A,* Vol. 82, 1909, pp. 546-559.

[33] Poynting, J. H., "Changes in Dimensions of Steel Wire when Twisted and Pressure of Distortional Waves in Steel," *Proceedings of the Royal Society, London, Series A,* Vol. 86, 1912, pp. 543-561.

[34] Swift, H. W., "Length Changes in Metals under Torsional Overstrain," *Engineering*, Vol. 163, 1947, pp. 253-257.

[35] Wack, B., "The Torsion of Tube (or a Rod): General Cylindrical Kinematics and Some Axial Deformation and Ratchetting Measurements," *Acta Mechanica*, Vol. 80, 1989, pp. 39-59.

[36] Bonacuse, P. J. and Kalluri, S., "Cyclic Axial-Torsional Deformation Behavior of a Cobalt-Base Superalloy," *Cyclic Deformation, Fracture, and Nondestructive Evaluation of Advanced Materials: Second Volume,* ASTM STP 1184, M. R. Mitchell and O. Buck, Eds., American Society for Testing and Materials, 1994, pp. 204-229.

[37] Kalluri, S., McGaw, M. A., and Halford, G. R., "Fatigue Life Estimation under Cumulative Cyclic Loading Conditions," Paper Presented at the 31st National Symposium on Fatigue and Fracture Mechanics, June 22-24, 1999, Cleveland, Ohio.

Figure Captions

Fig. 1 -- Axial Fatigue Life Relationships for Haynes 188 at 538°C

Fig. 2 -- Torsional Fatigue Life Relationships for Haynes 188 at 538°C

Fig. 3 -- Estimation of Torsional Fatigue Lives with Modified Multiaxiality Factor Approach

Fig. 4 -- Cyclic Stress Evolution in Baseline Fatigue Tests

a) Axial Tests

b) Torsional Tests

Fig. 5 -- Cyclic Stress Evolution at the Second Load-Level in Cumulative Fatigue Tests

a) Axial/Axial Tests

b) Torsional/Torsional Tests

c) Axial/Torsional Tests

d) Torsional/Axial Tests

Fig. 6 -- Fatigue Life Estimation of Two Load-Level Cumulative Fatigue Tests

a) Axial/Axial Tests

b) Torsional/Torsional Tests

c) Axial/Torsional Tests

d) Torsional/Axial Tests

Fig. 7 – Comparison of the Summation of Life Fractions in Two Load-Level Cumulative Fatigue Tests

a) Axial/Axial Tests

b) Torsional/Torsional Tests

c) Axial/Torsional Tests

d) Torsional/Axial Tests

Fig. 8 -- Comparison of Remaining Cyclic Lives in the Axial and Torsional Cumulative Fatigue Tests

a) Linear Damage Rule

b) Damage Curve Approach

TABLE 1 – Axial Fatigue Data of Haynes 188 at 538°C

Specimen Number	ν (Hz)	$\Delta\varepsilon$	$\Delta\sigma$ (MPa)	σ_m (MPa)	$\Delta\varepsilon_{el}$	$\Delta\varepsilon_{in}$	N_f (Cycles)	Crack Orientation[a]
HYII5	0.1	0.0202	1 274	-14	0.0067	0.0135	787	90°
HYII6	0.1	0.0202	1 266	-12	0.0067	0.0135	864	90°
HYII78	0.1	0.0143	1 137	-12	0.0060	0.0083	1 639	90°
HYII77	0.1	0.0102	1 011	-11	0.0053	0.0049	4 755	90°
HYII10	0.5	0.0071	937	-16	0.0049	0.0022	24 105	90°
HYII11	0.5	0.0071	980	-20	0.0052	0.0019	24 030	90°
HYII14	0.5	0.0067	955	-18	0.0050	0.0017	35 889	80°
HYII15	0.5	0.0067	962	-19	0.0051	0.0016	42 937	80°
HYII13	0.5	0.0060	1056	-22	0.0056	0.0004	252 351[b]	...

[a]Measured with specimen's axis as the reference (0°)
[b]Runout (No cracks were observed)

TABLE 2 – Torsional Fatigue Data of Haynes 188 at 538°C

Specimen Number	ν (Hz)	$\Delta\gamma$	$\Delta\tau$ (MPa)	τ_m (MPa)	$\Delta\gamma_{el}$	$\Delta\gamma_{in}$	N_f (Cycles)	Crack Orientation[a]
HYII1	0.1	0.0346	737	2	0.0101	0.0245	1 630	0°
HYII2	0.1	0.0345	727	1	0.0100	0.0245	1 882	0°
HYII79	0.1	0.0217	625	0	0.0086	0.0131	4 023	0°
HYII17	0.5	0.0139	579	0	0.0079	0.0060	19 080	0°
HYII21	0.5	0.0130	571	0	0.0078	0.0052	20 762	0°
HYII20	0.5	0.0130	607	0	0.0083	0.0047	43 678	0°
HYII23	0.5	0.0122	610	1	0.0084	0.0038	52 280	0°
HYII7	0.5	0.0121	603	0	0.0083	0.0038	65 612	0°
HYII16	0.5	0.0101	624	0	0.0085	0.0016	250 475[b]	...
HYII4	0.5	0.0095	629	0	0.0086	0.0009	367 447[b]	...
HYII16	0.5	0.0073	527	-2	0.0072	0.0001	550 183[b]	...

[a]Measured with specimen's axis as the reference (0°)
[b]Runout (No cracks were observed)

TABLE 3 – Constants for Axial and Torsional Fatigue Life Relationships

Constants	Axial Life Relation	Constants	Torsional Life Relation
b	- 0.08	b_T	- 0.082
c	- 0.544	c_T	- 0.534
B	0.0113	B_T	0.0187
C	0.501	C_T	1.24

TABLE 4 – Axial and Torsional Interaction Fatigue Data of Haynes 188 at 538°C

Specimen Number	First Load Level ; ν = 0.1 Hz							Second Load Level ; ν = 0.5 Hz							Crack Orientation[a]
	$\Delta\varepsilon_1$	$\Delta\sigma_1$ (MPa)	σ_{m1} (MPa)	$\Delta\gamma_1$	$\Delta\tau_1$ (MPa)	τ_{m1} (MPa)	n_1 (Cycles)	$\Delta\varepsilon_2$	$\Delta\sigma_2$ (MPa)	σ_{m2} (MPa)	$\Delta\gamma_2$	$\Delta\tau_2$ (MPa)	τ_{m2} (MPa)	n_2 (Cycles)	
HYII75	0.0205	1 138	-10	...	...	...	83	0.0065	1 015	-5	...	...	...	17 923	90°
HYII64	0.0202	1 230	-12	...	...	...	165	0.0065	1 035	-6	...	...	...	10 540	75°
HYII65	0.0201	1 276	-11	...	...	...	330	0.0065	1 055	-7	...	...	...	8 306	75°
HYII70	0.0200	1 256	-13	...	...	...	495	0.0064	1 054	-5	...	...	...	4 857	60°[b]
HYII76	...	...	...	0.0347	711	1	175	...	...	...	0.0122	646	0	59 143	0°
HYII66	...	...	...	0.0352	739	1	350	...	...	...	0.0122	650	0	29 547	0°
HYII67	...	...	...	0.0349	738	1	700	...	...	...	0.0122	652	0	4 156	85°
HYII71	...	...	...	0.0345	753	3	1 051	...	...	...	0.0122	646	-1	951	90°
HYII73	0.0202	1 154	-12	...	...	...	83	...	...	...	0.0121	652	1	14 732	75°[b]
HYII8	0.0205	1 255	-14	...	...	...	165	...	...	...	0.0122	679	2	17 033	0°
HYII61	0.0202	1 256	-12	...	...	...	330	...	...	...	0.0122	689	2	9 919	75°
HYII68	0.0203	1 252	-13	...	...	...	495	...	...	...	0.0122	683	3	11 700	90°
HYII74	...	...	...	0.0349	722	1	175	0.0062	1 152	0	...	...	...	28 980	75°
HYII62	...	...	...	0.0349	731	-1	350	0.0064	1 162	2	...	...	...	18 380	80°
HYII63	...	...	...	0.0346	751	1	700	0.0064	1 179	5	...	...	...	8 799	90°
HYII72	...	...	...	0.0345	749	-1	1 051	0.0063	1 143	-4	...	...	...	4 642	90°
HYII69	...	...	...	0.0345	760	0	1 151	0.0062	1 162	6	...	...	...	2 824	80°

[a]Measured with specimen's axis as the reference(0°)

[b]Initial orientation; crack eventually changed to 90° orientation

TABLE 5 – Comparison of Life Fractions for Axial and Torsional Cumulative Fatigue Tests

Specimen Number	Test Type	Applied Life Fraction, (n_1/N_1)	Remaining Life Fraction, (n_2/N_2)			Sum of Life Fractions, $(n_1/N_1) + (n_2/N_2)$		
			LDR	DCA	Experiment	LDR	DCA	Experiment
HYII75	Axial/Axial	0.101	0.899	0.387	0.457	1.000	0.488	0.558
HYII64	Axial/Axial	0.200	0.800	0.291	0.269	1.000	0.491	0.469
HYII65	Axial/Axial	0.400	0.600	0.178	0.212	1.000	0.578	0.612
HYII70	Axial/Axial	0.600	0.400	0.103	0.124	1.000	0.703	0.724
HYII76	Torsional/Torsional	0.100	0.900	0.432	1.010	1.000	0.532	1.110
HYII66	Torsional/Torsional	0.200	0.800	0.327	0.504	1.000	0.527	0.704
HYII67	Torsional/Torsional	0.400	0.600	0.202	0.071	1.000	0.602	0.471
HYII71	Torsional/Torsional	0.600	0.400	0.118	0.016	1.000	0.718	0.616
HYII73	Axial/Torsional	0.101	0.899	0.341	0.252	1.000	0.442	0.353
HYII8	Axial/Torsional	0.200	0.800	0.254	0.291	1.000	0.454	0.491
HYII61	Axial/Torsional	0.400	0.600	0.153	0.169	1.000	0.553	0.569
HYII68	Axial/Torsional	0.600	0.400	0.089	0.200	1.000	0.689	0.800
HYII74	Torsional/Axial	0.100	0.900	0.470	0.661	1.000	0.570	0.761
HYII62	Torsional/Axial	0.200	0.800	0.358	0.419	1.000	0.558	0.619
HYII63	Torsional/Axial	0.400	0.600	0.223	0.201	1.000	0.623	0.601
HYII72	Torsional/Axial	0.600	0.400	0.131	0.106	1.000	0.731	0.706
HYII69	Torsional/Axial	0.657	0.343	0.109	0.064	1.000	0.766	0.721

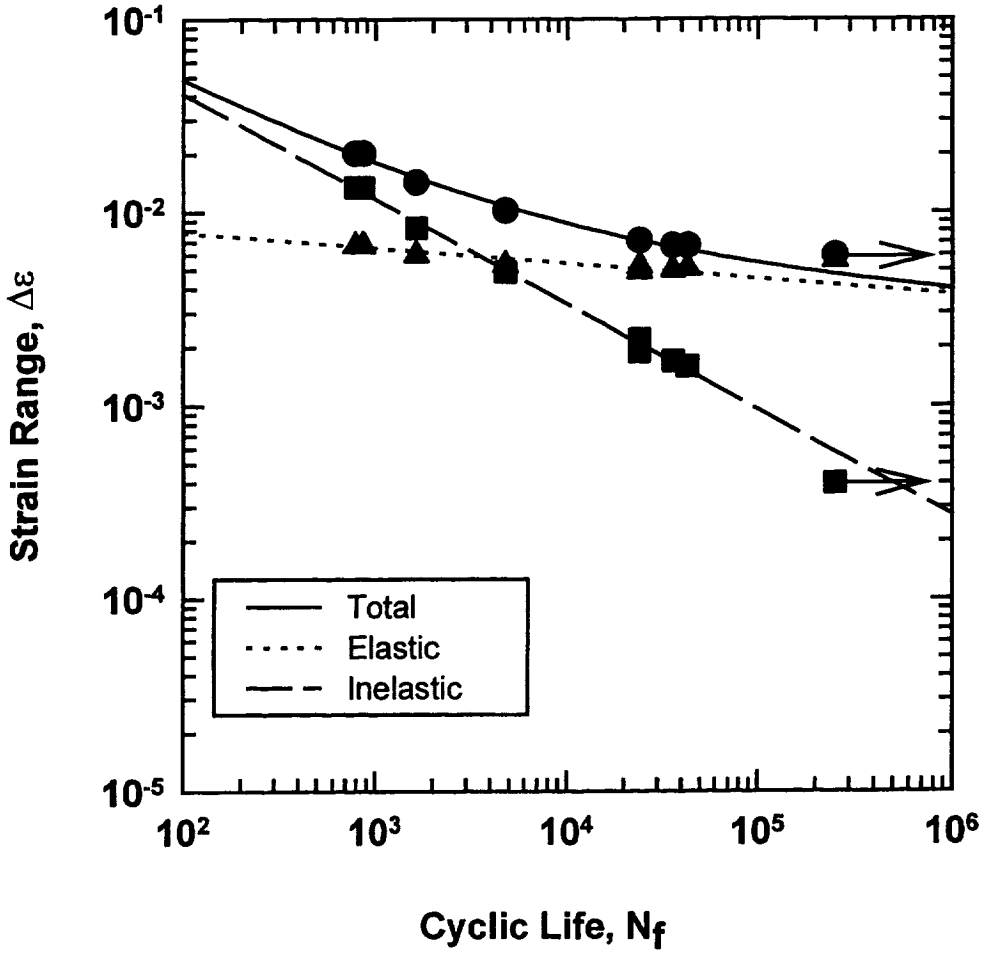

Fig. 1 -- Axial Fatigue Life Relationships for Haynes 188 at 538°C

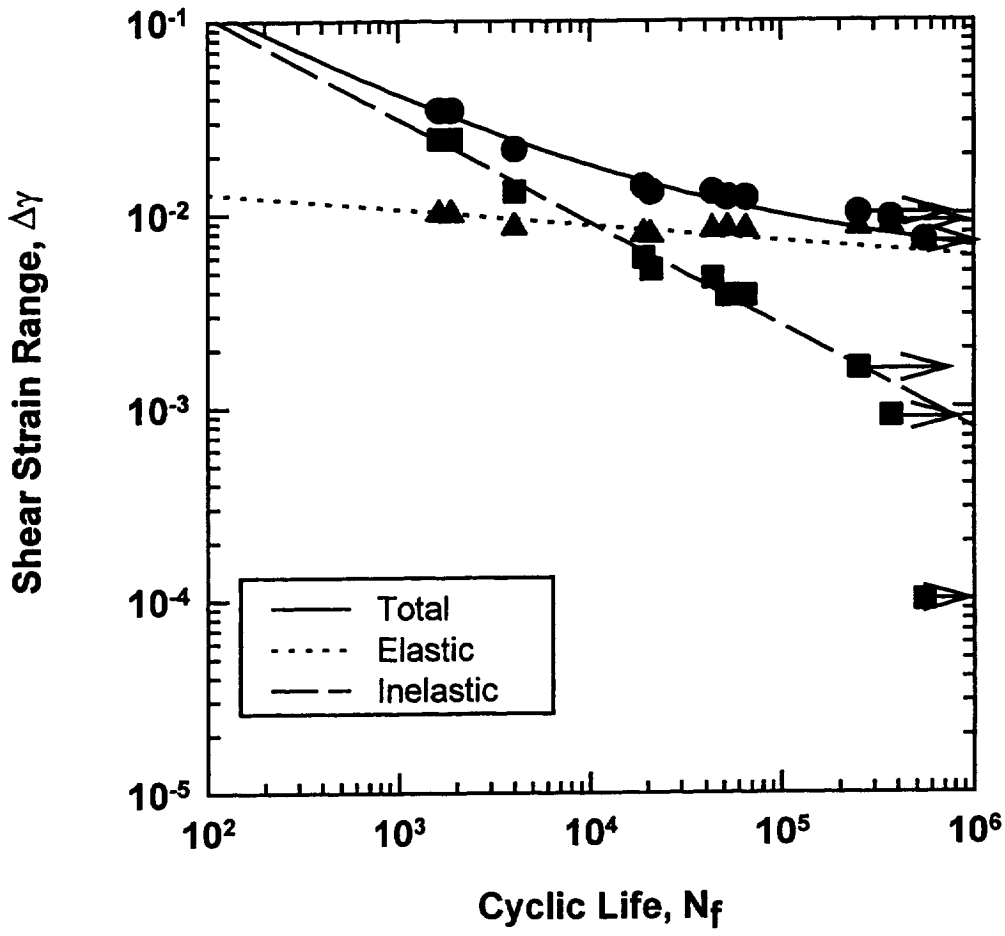

Fig. 2 -- Torsional Fatigue Life Relationships for Haynes 188 at 538°C

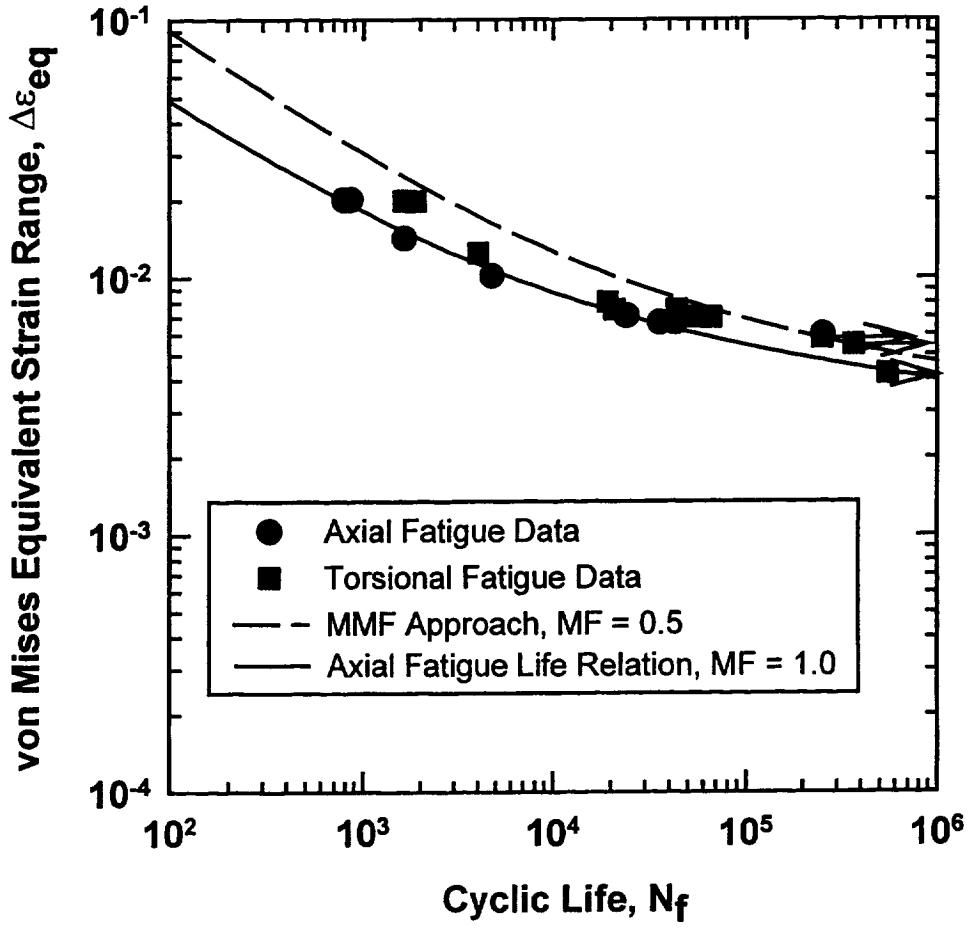

Fig. 3 -- Estimation of Torsional Fatigue Lives with Modified Multiaxiality Factor Approach

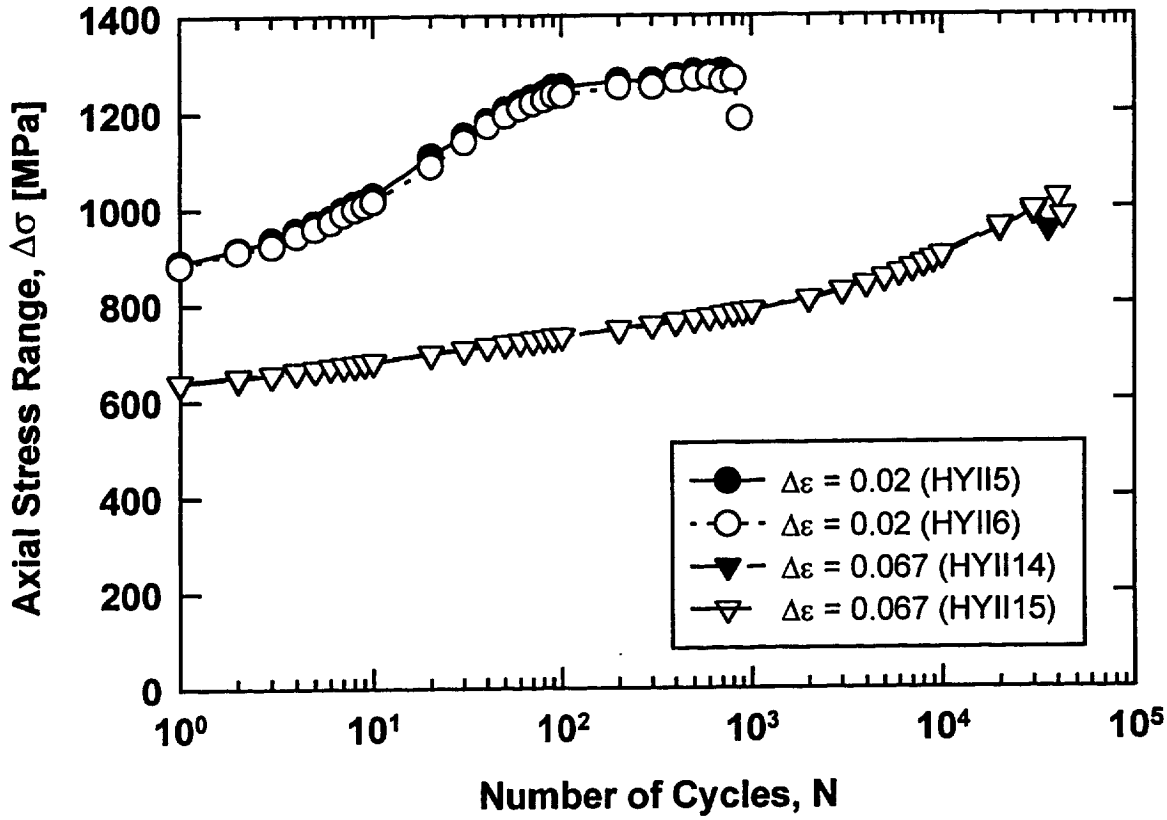

a) Axial Tests

Fig. 4 -- Cyclic Stress Evolution in Baseline Fatigue Tests

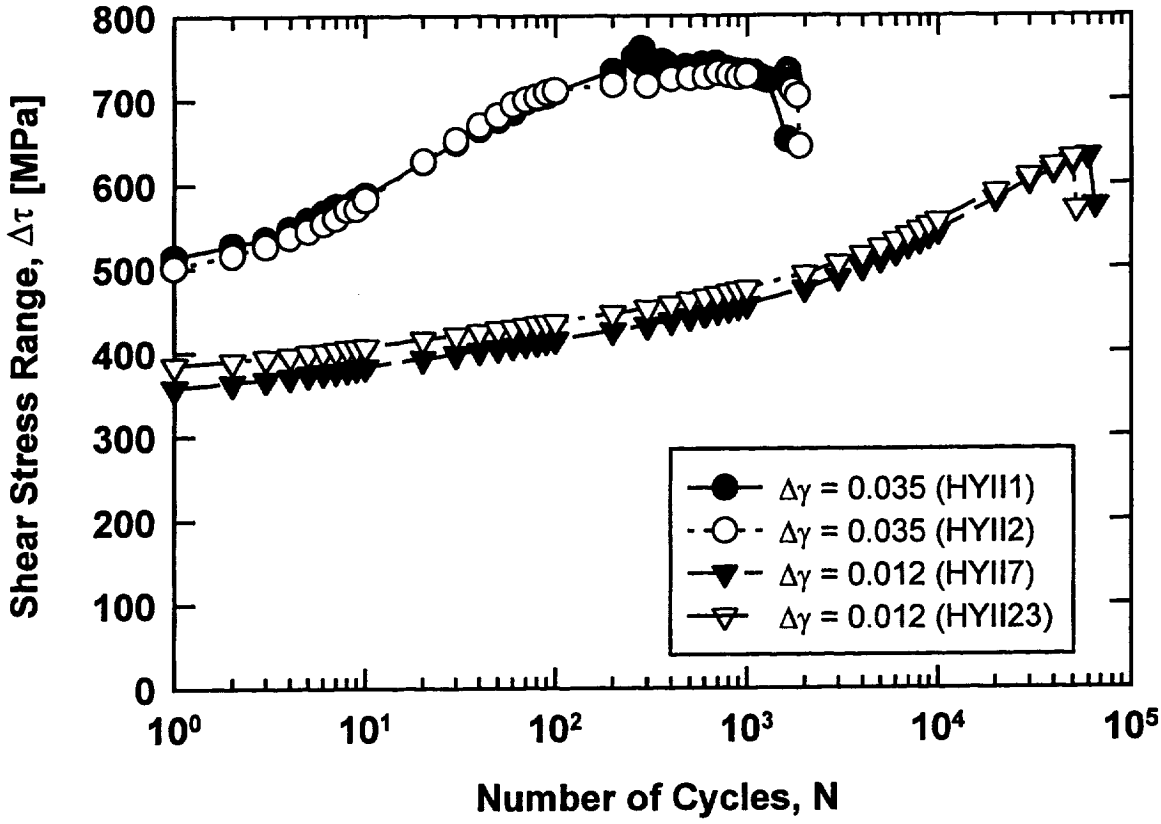

b) Torsional Tests

Fig. 4 -- Cyclic Stress Evolution in Baseline Fatigue Tests

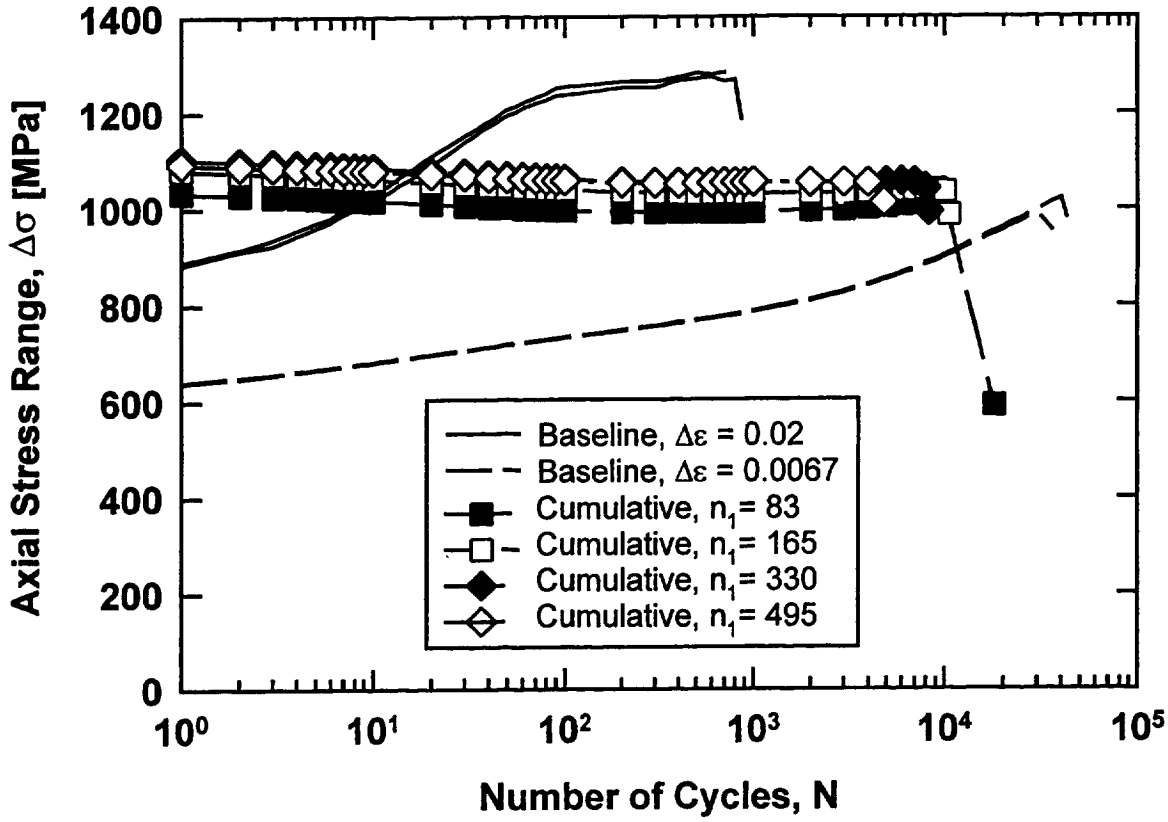

a) Axial/Axial Tests

Fig. 5 -- Cyclic Stress Evolution at the Second Load-Level in Cumulative Fatigue Tests

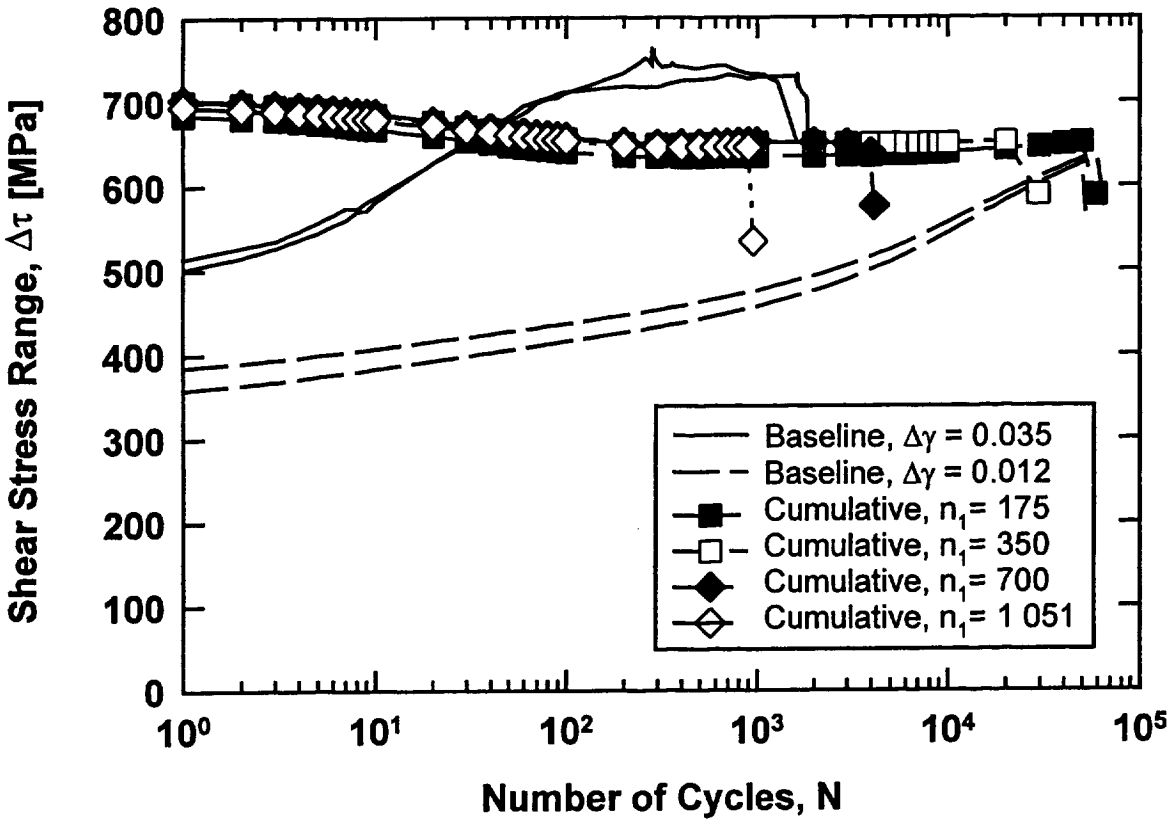

b) Torsional/Torsional Tests

Fig. 5 -- Cyclic Stress Evolution at the Second Load-Level in Cumulative Fatigue Tests

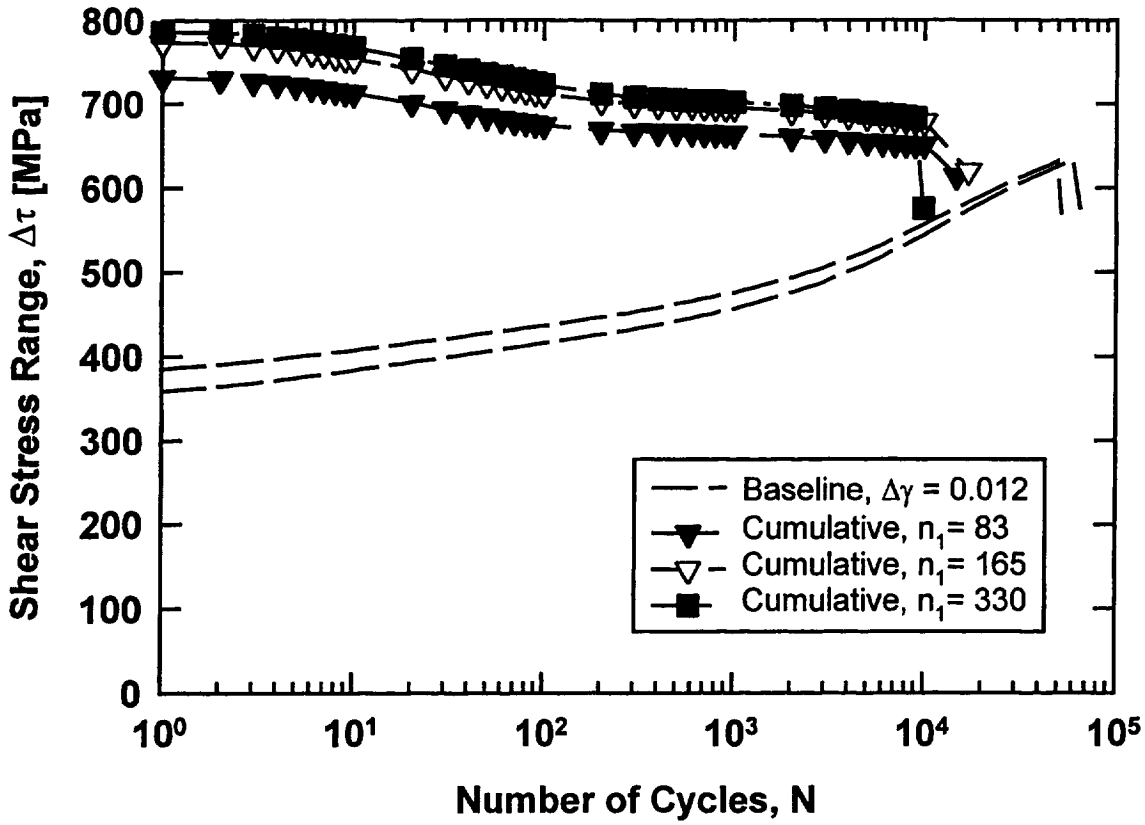

c) Axial/Torsional Tests

Fig. 5 -- Cyclic Stress Evolution at the Second Load-Level in Cumulative Fatigue Tests

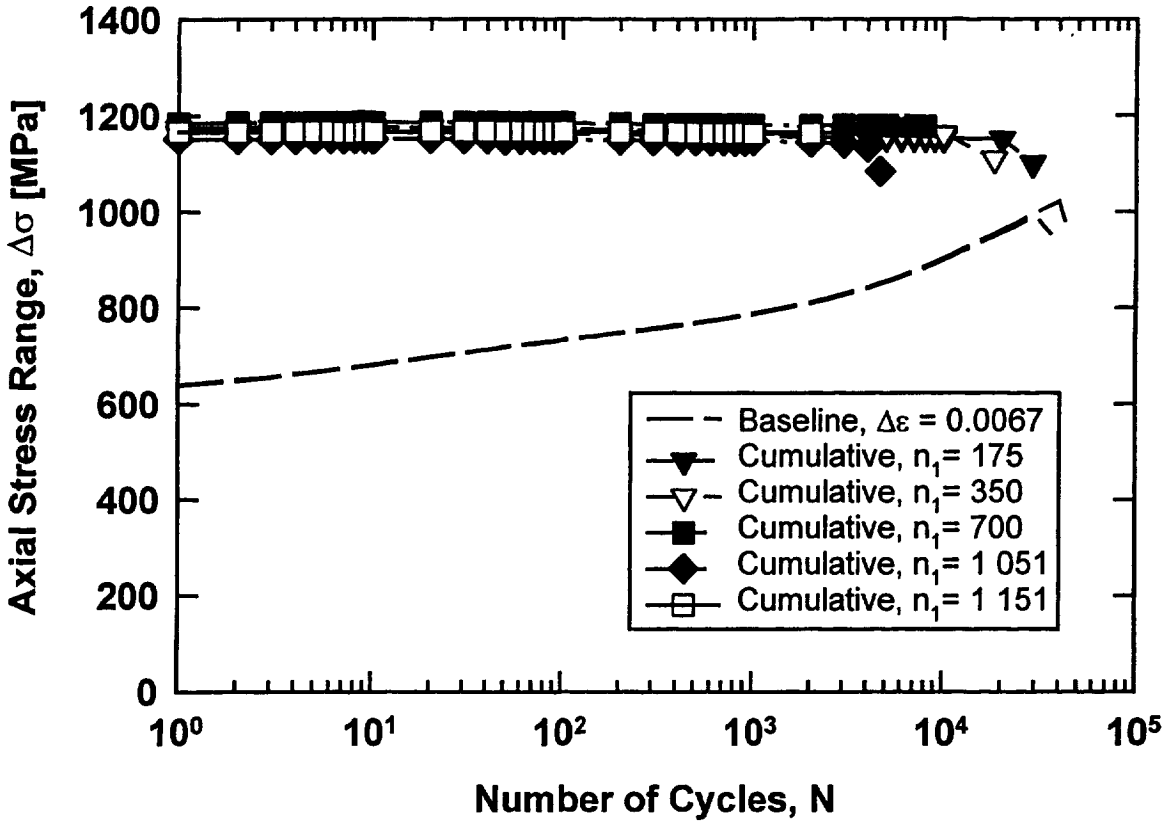

d) Torsional/Axial Tests

Fig. 5 -- Cyclic Stress Evolution at the Second Load-Level in Cumulative Fatigue Tests

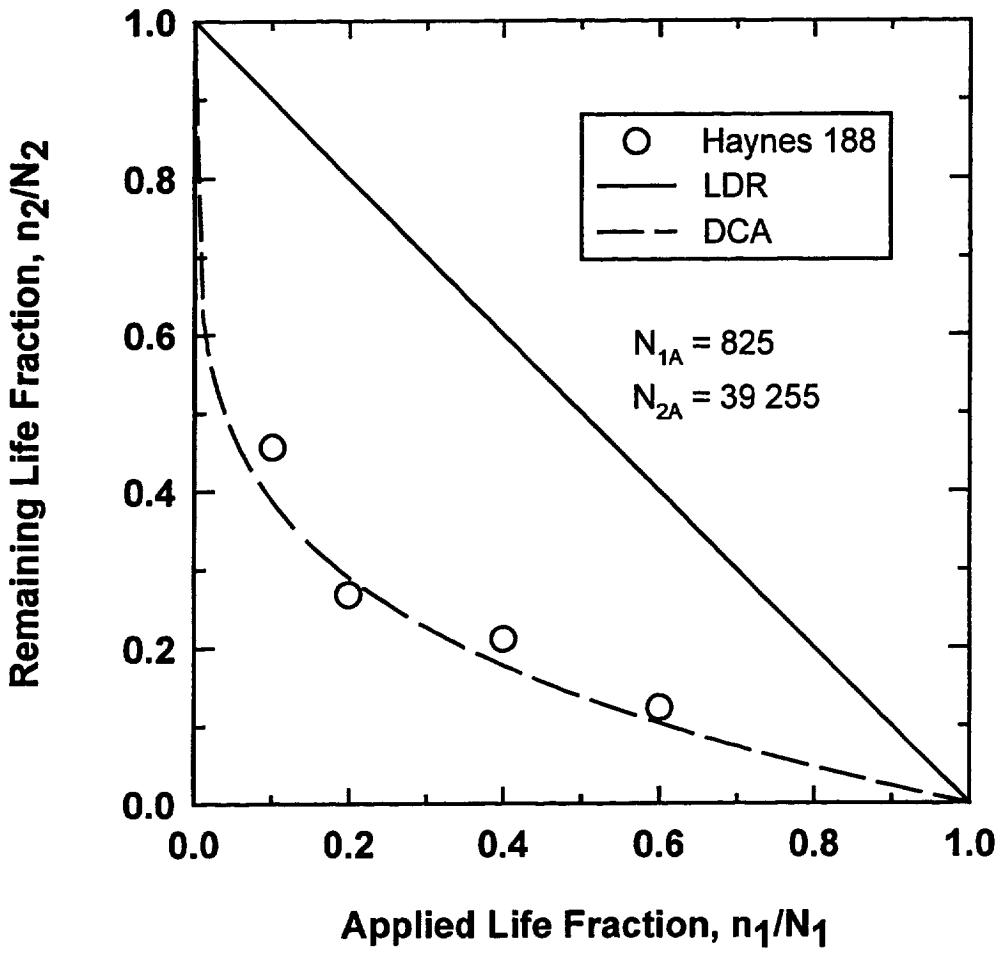

a) Axial/Axial Tests

Fig. 6 -- Fatigue Life Estimation of Two Load-Level Cumulative Fatigue Tests

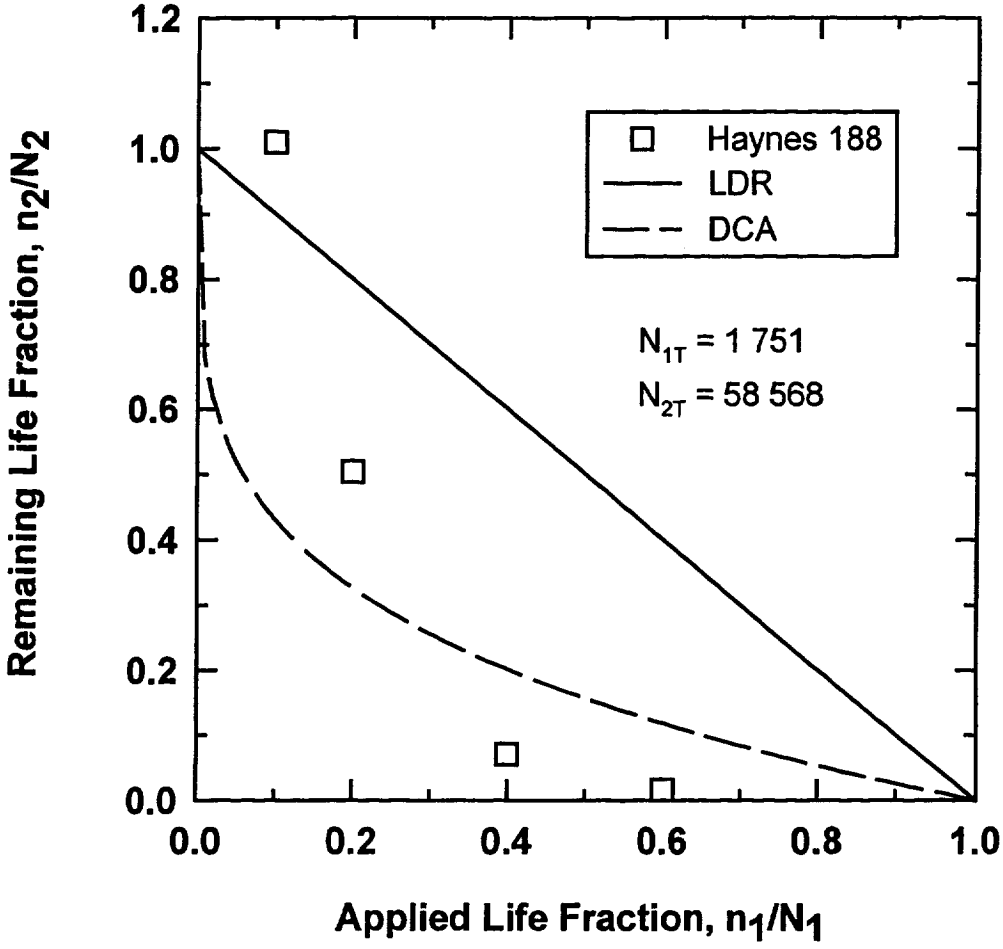

b) Torsional/Torsional Tests

Fig. 6 -- Fatigue Life Estimation of Two Load-Level Cumulative Fatigue Tests

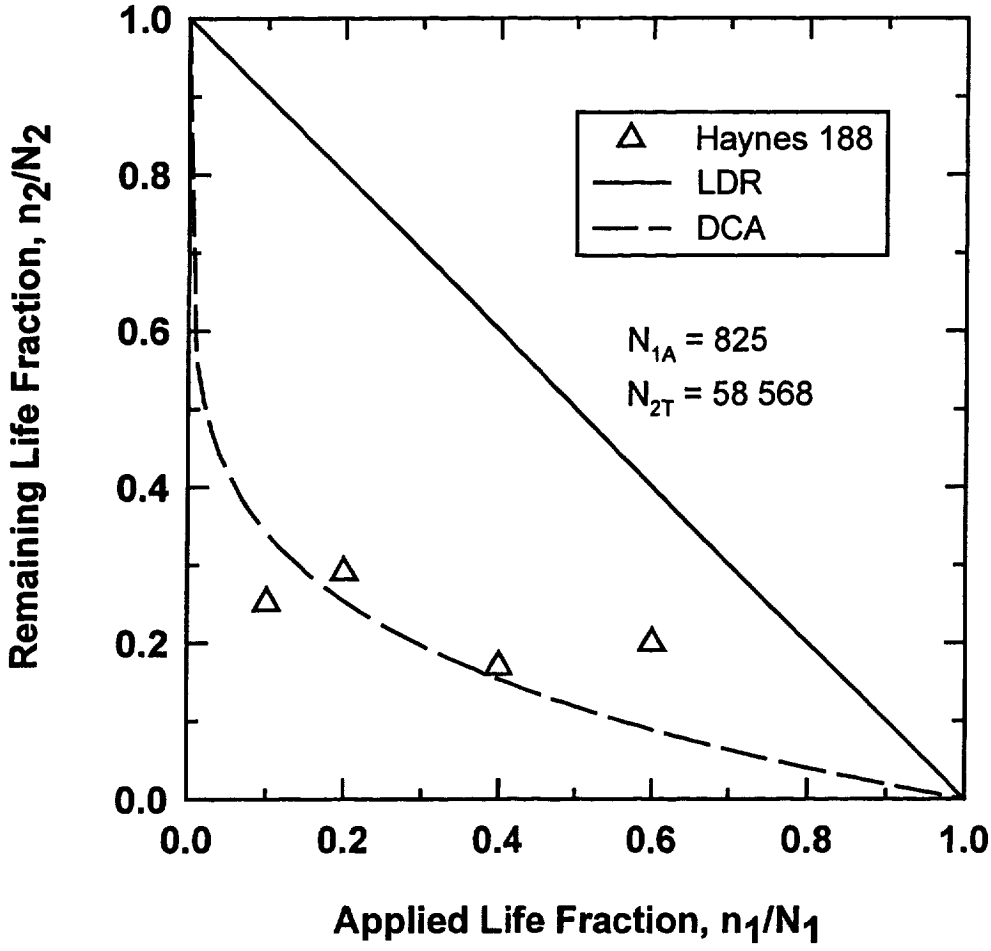

c) Axial/Torsional Tests

Fig. 6 -- Fatigue Life Estimation of Two Load-Level Cumulative Fatigue Tests

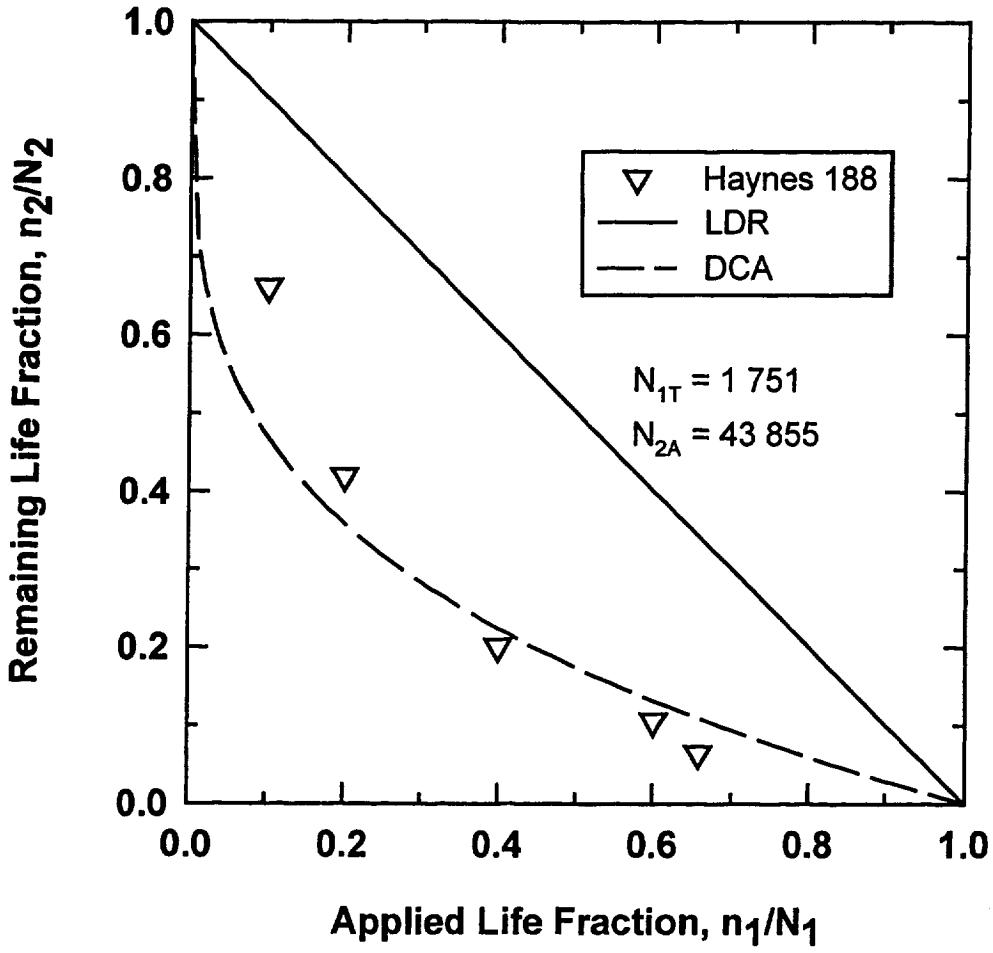

d) Torsional/Axial Tests

Fig. 6 -- Fatigue Life Estimation of Two Load-Level Cumulative Fatigue Tests

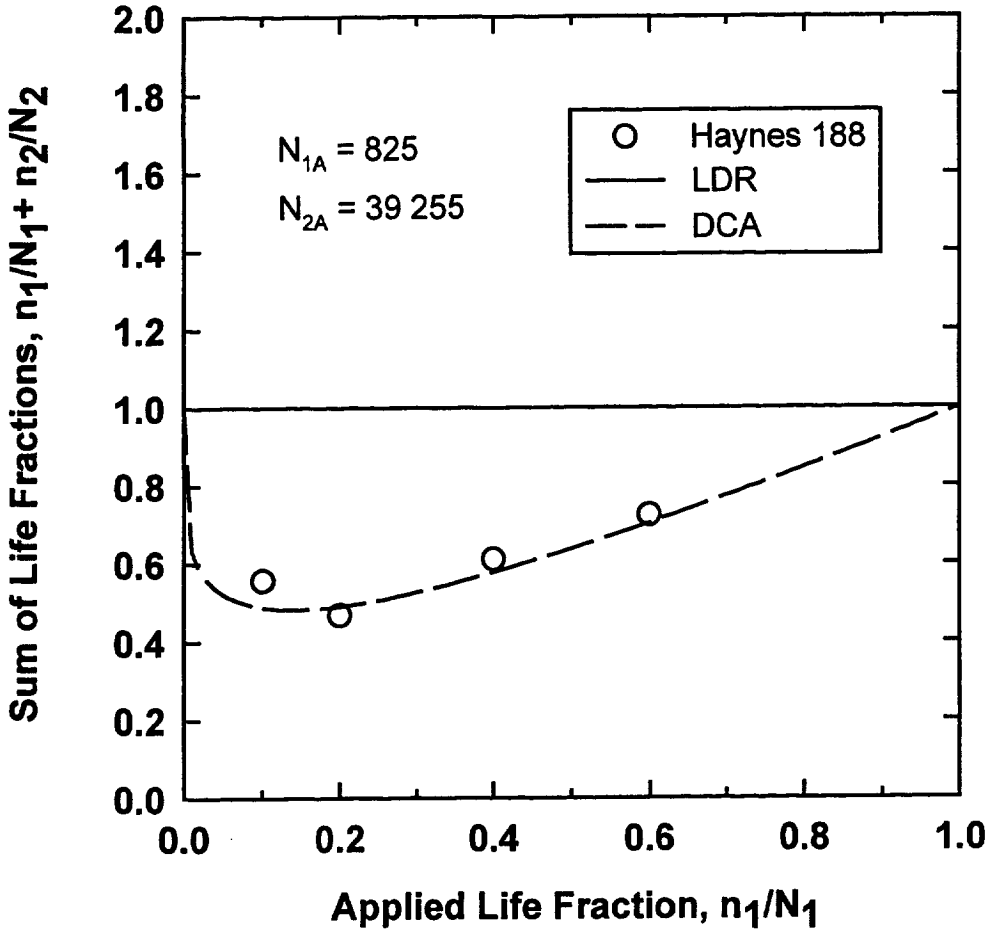

a) Axial/Axial Tests

Fig. 7 -- Comparison of the Summation of Life Fractions in Two Load-Level Cumulative Fatigue Tests

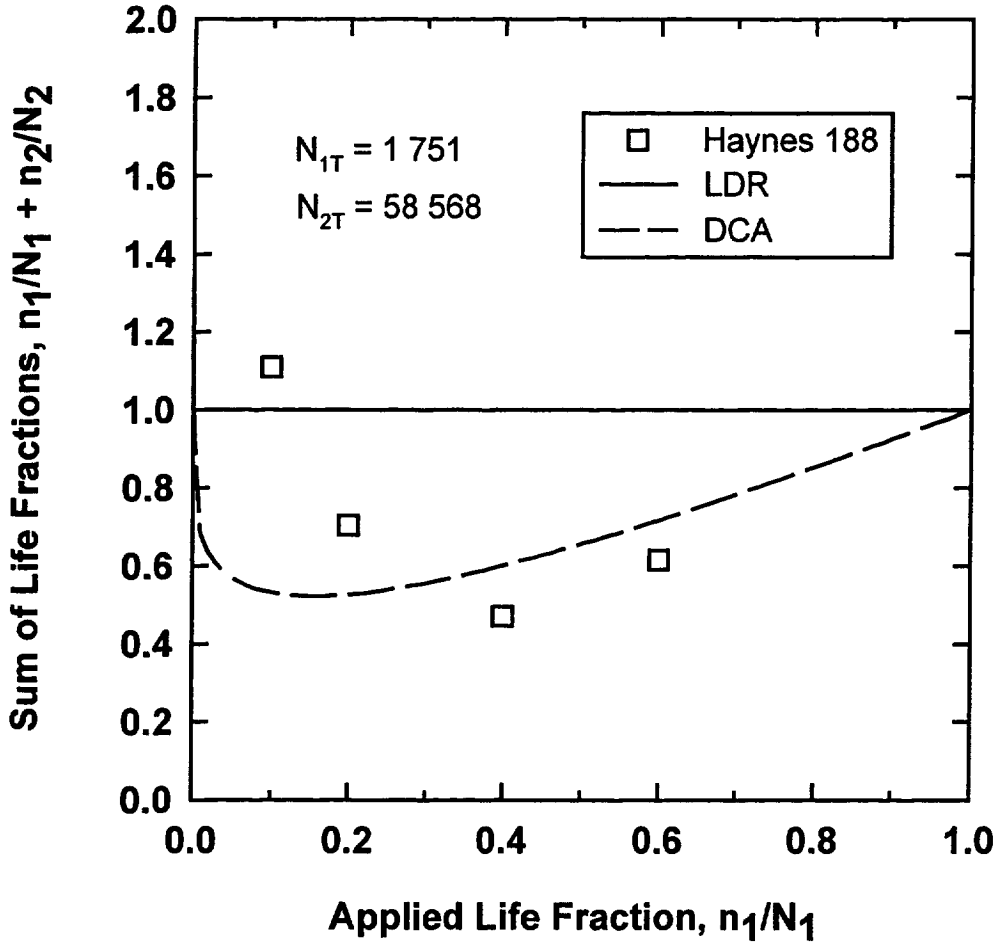

b) Torsional/Torsional Tests

Fig. 7 -- Comparison of the Summation of Life Fractions in Two Load-Level Cumulative Fatigue Tests

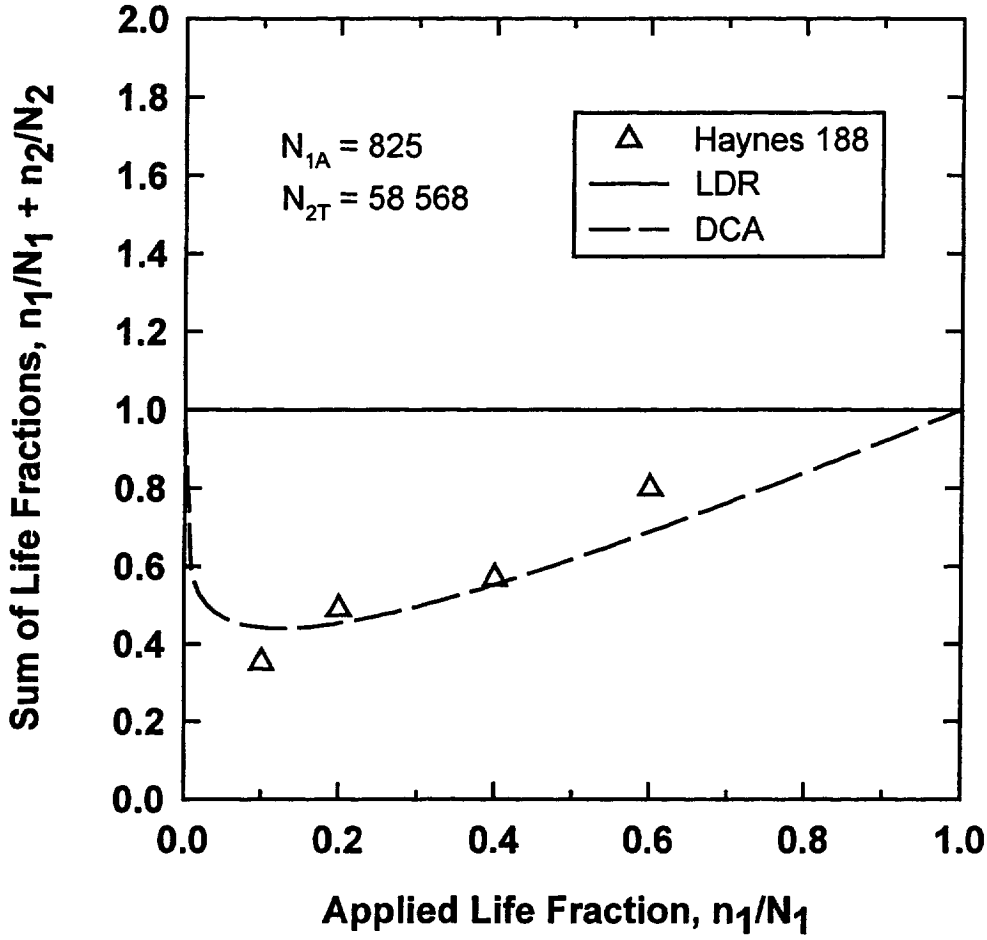

c) Axial/Torsional Tests

Fig. 7 -- Comparison of the Summation of Life Fractions in Two Load-Level Cumulative Fatigue Tests

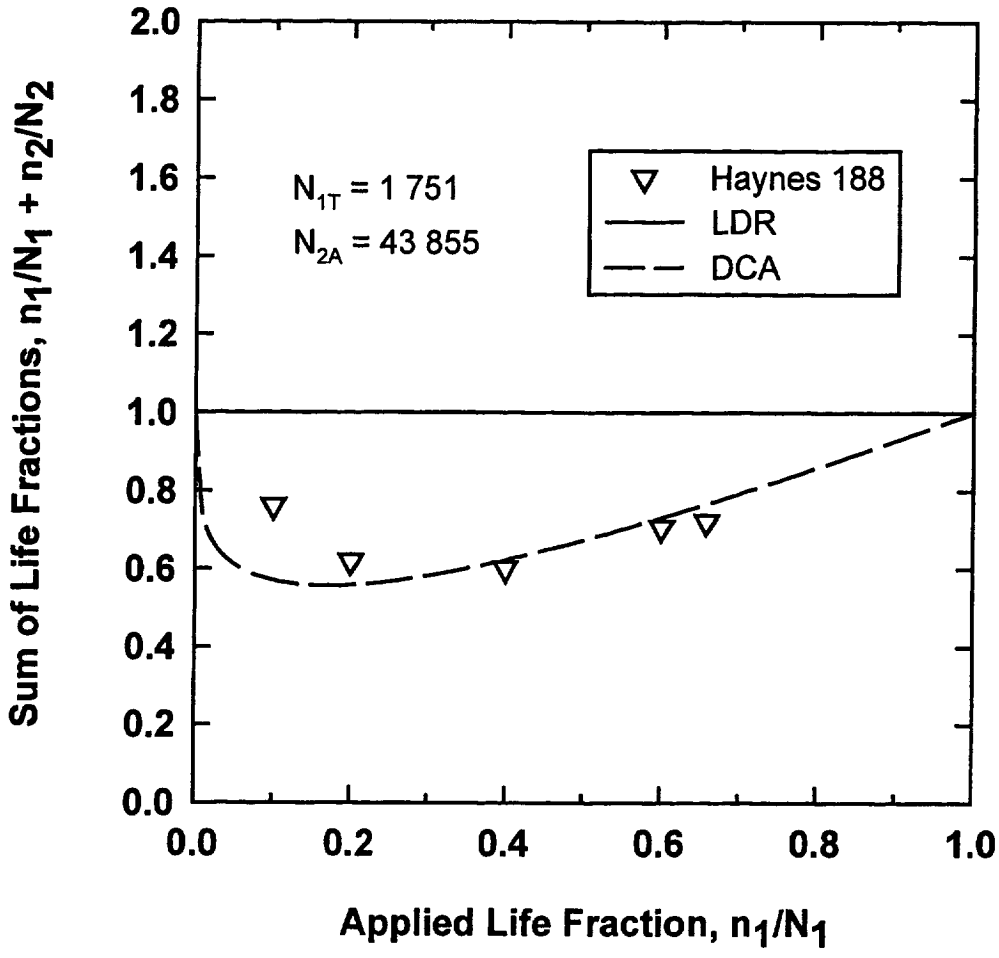

d) Torsional/Axial Tests

Fig. 7 -- Comparison of the Summation of Life Fractions in Two Load-Level Cumulative Fatigue Tests

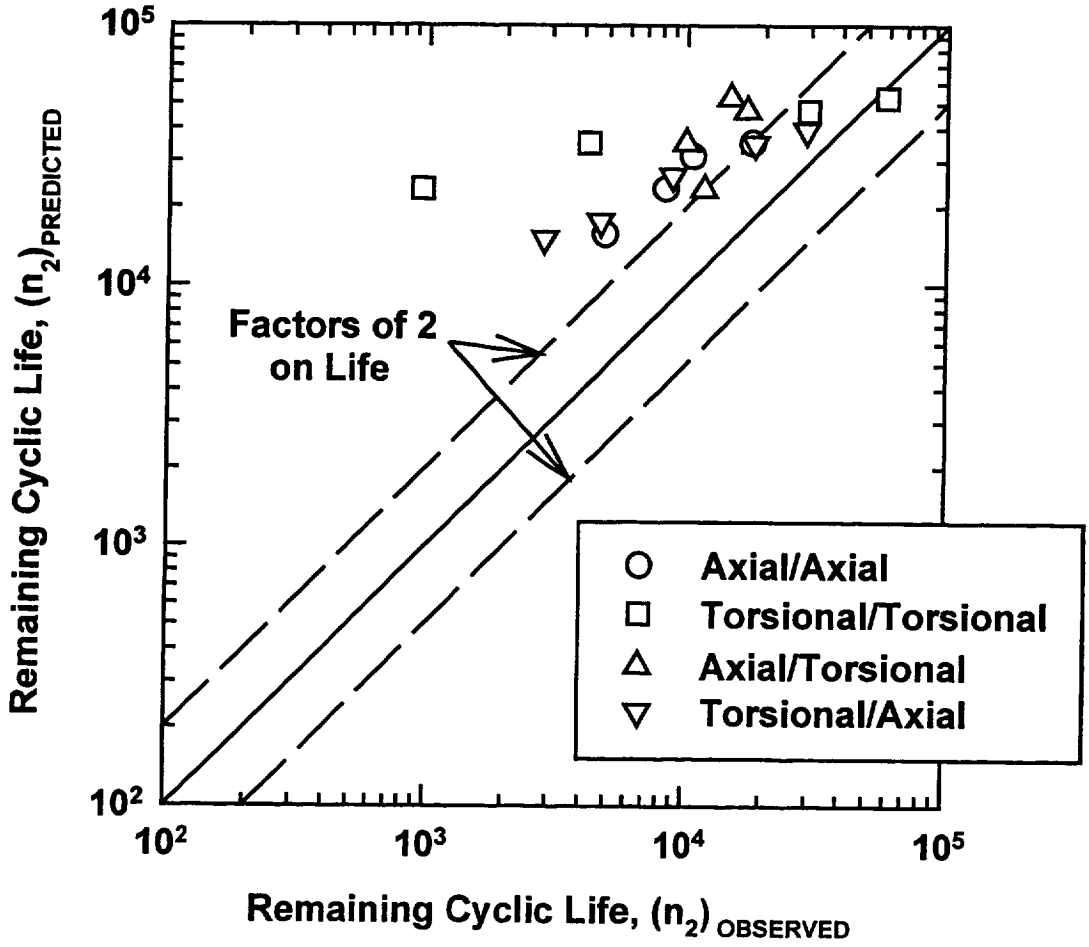

a) Linear Damage Rule

Fig. 8 -- Comparison of Remaining Cyclic Lives in the Axial and Torsional Cumulative Fatigue Tests

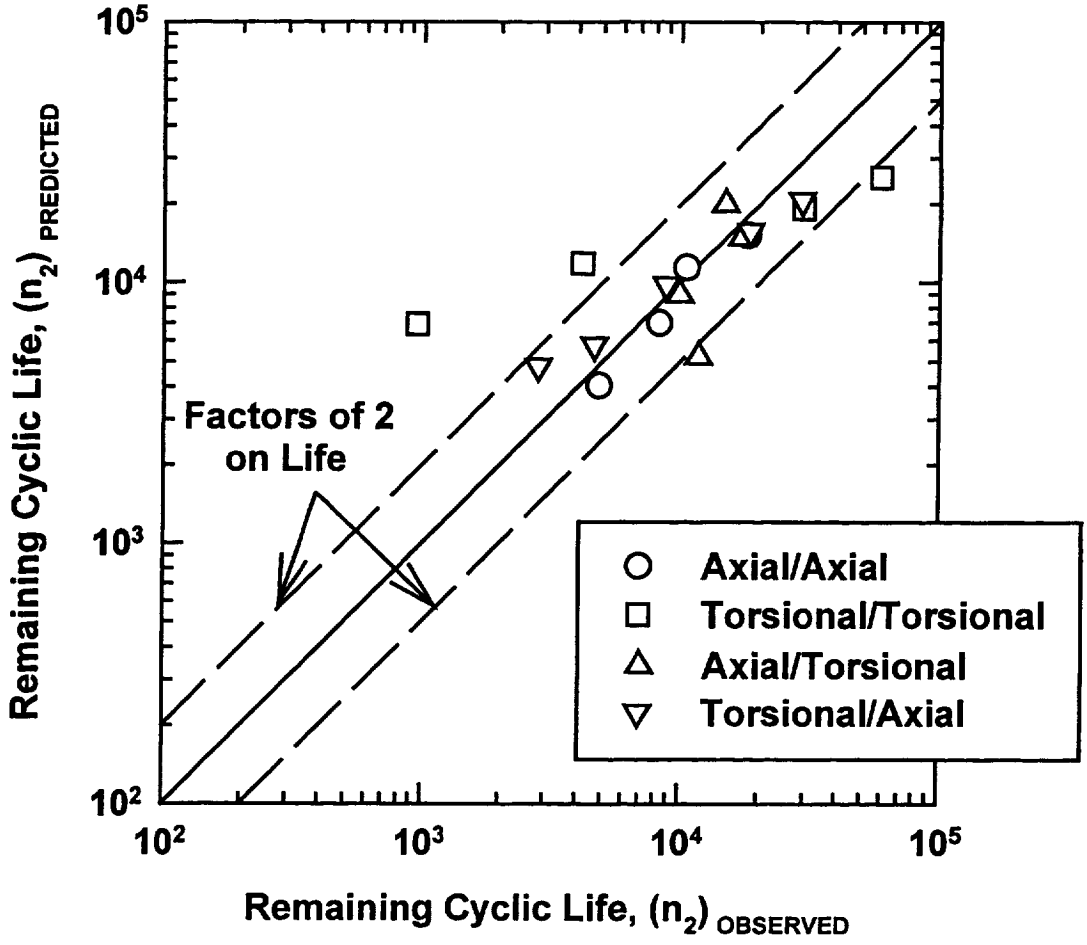

b) Damage Curve Approach

Fig. 8 -- Comparison of Remaining Cyclic Lives in the Axial and Torsional Cumulative Fatigue Tests